J. Biochem. 2009;146(2)173–183
doi:10.1093/jb/mvp059

Thermodynamic and Kinetic Effects of Morpholino Modification on Pyrimidine Motif Triplex Nucleic Acid Formation under Physiological Condition

Hidetaka Torigoe*, Kiyomi Sasaki and Takuma Katayama

Department of Applied Chemistry, Faculty of Science, Tokyo University of Science, 1-3 Kagurazaka, Shinjuku-ku, Tokyo 162-8601, Japan

Received December 13, 2008; accepted March 23, 2009; published online April 7, 2009

Due to instability of pyrimidine motif triplex nucleic acid under physiological pH and low magnesium ion concentration, stabilization of the triplex under the physiological condition is crucial in improving its therapeutic potential to artificially control gene expression *in vivo*. To this end, we investigated the thermodynamic and kinetic effects of morpholino (MOR) modification of triplex-forming oligonucleotide (TFO) on the triplex formation under the physiological condition. The thermodynamic analyses indicated that the MOR modification of TFO not only significantly increased the thermal stability of the triplex but also increased the binding constant for the triplex formation by nearly 2 orders of magnitude. The consideration of the observed thermodynamic parameters suggested that the increased rigidity of the MOR-modified TFO in the free state relative to the corresponding unmodified TFO may enable the significant increase in the binding constant. Kinetic data demonstrated that the observed increase in the binding constant resulted from the considerable increase in the association rate constant rather than the decrease in the dissociation rate constant. This information will be valuable for designing novel chemically modified TFO with higher binding affinity in the triplex formation under physiological conditions, leading to progress in therapeutic applications of the antigene strategy *in vivo*.

Key words: triplex nucleic acid, triplex-forming oligonucleotide, morpholino modification, isothermal titration calorimetry, interaction analysis system.

Abbreviations: TFO, triplex-forming oligonucleotide; MOR, morpholino; PO, natural phosphodiester; Bt, biotinylated; EMSA, electrophoretic mobility shift assay; T_m, melting temperature; CD, circular dichroism; ITC, isothermal titration calorimetry; IAsys, interaction analysis system; k_{on}, on-rate constant; k_{assoc}, association rate constant; k_{off}, off-rate constant; k_{dissoc}, dissociation rate constant.

In recent years, triplex nucleic acid has attracted considerable interest because of its possible biological functions *in vivo* and its wide variety of potential applications, such as regulation of gene expression by antigene technologies, site-specific cleavage of duplex DNA, mapping of genomic DNA, and gene-targeted mutagenesis (*1–5*). A triplex nucleic acid is usually formed through the sequence-specific interaction between a single-stranded homopyrimidine or homopurine triplex-forming oligonucleotide (TFO) and the major groove of homopurine-homopyrimidine stretch in duplex DNA (*3*, *4*). In the pyrimidine motif triplex, a homopyrimidine TFO binds parallel to the homopurine strand of the target duplex by Hoogsteen hydrogen bonding to form T•A:T and C^+•G:C base triplets (*3*, *4*). On the other hand, in the purine motif triplex, a homopurine TFO binds antiparallel to the homopurine strand of the target duplex by reverse Hoogsteen hydrogen bonding to form A•A:T (or T•A:T) and G•G:C base triplets (*3*, *4*).

As protonation of the cytosine bases in a homopyrimidine TFO is required to bind with the guanine bases of the G:C target duplex, the formation of the pyrimidine motif triplex needs an acidic pH condition and is thus extremely unstable at physiological neutral pH (*6–8*). On the other hand, the pH-independent formation of the purine motif triplex is available at neutral pH. However, the purine motif triplex formation is severely inhibited by physiological concentrations of certain monovalent cations, especially K^+ (*9*, *10*). Undefined association between K^+ and the guanine-rich homopurine TFO has been applied to explain the inhibitory effect (*9*, *10*). Thus, stabilization of the pyrimidine motif triplex at neutral pH is quite necessary for improving the therapeutic potential of the triplex to artificially regulate gene expression *in vivo* as antigene technologies. Replacement of the cytosine bases in a homopyrimidine TFO with 5-methylcytosine (*7*, *11–13*) or other chemically modified base analogues (*14–18*), and conjugation of different DNA intercalators to TFO (*19*, *20*) have been used to overcome the requirement of an acidic pH for the pyrimidine motif triplex formation and to stabilize the pyrimidine motif triplex at neutral pH. In addition, electrostatic repulsion between TFO and the target duplex caused by excess

*To whom correspondence should be addressed.
Tel: +81-3-5228-8259, Fax: +81-3-5261-4631,
E-mail: htorigoe@rs.kagu.tus.ac.jp

(a)

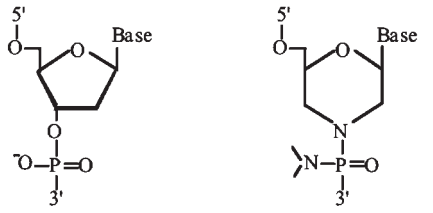

(b)

```
Pyr15T       5'-CTCTTCTTTTCTTTC-3'(backbone:PO)
Pyr15MOR     5'-CTCTTCTTTTCTTTC-3'(backbone:MOR)
Pur23A  5'-GCGCGAGAAGAAAAGAAAGCCGG-3'
Pyr23T  3'-CGCGCTCTTCTTTTCTTTCGGCC-5'
Pyr15NS      5'-TCTCCTCCCCTCCCT-3'
```

Fig. 1. **(a) Structural formulas for phosphodiester (PO) and morpholino (MOR) backbones.** (b) Oligonucleotide sequences for the target duplex (Pur23A•Pyr23T), the specific TFOs (Pyr15T and Pyr15MOR), and the non-specific TFO (Pyr15NS).

accumulation of phosphate anions upon the triplex formation produces extreme instability of the pyrimidine motif triplex (*21*, *22*). To reduce the electrostatic repulsion upon the triplex formation, most of *in vitro* triplex formation experiments were performed in the presence of high concentration (5–10 mM) of magnesium ion. However, low concentration (~0.8 mM) of magnesium ion was observed in the cell (*23*). Therefore, stabilization of the pyrimidine motif triplex under the low concentration of magnesium ion is crucial in improving the therapeutic potential of the triplex. Development of non-charged backbone linkages have been made to reduce the electrostatic repulsion upon the pyrimidine motif triplex formation and to improve the stability of the pyrimidine motif triplex under the low concentration of magnesium ion (*24–27*).

As part of the search for non-charged backbone modifications, morpholino (MOR) linkages (Fig. 1a) have been designed (*28–30*). Due to excellent hybridization properties towards RNA, MOR-modified oligonucleotides have been widely used as anti-sense agents to inhibit translation of target mRNA, especially in anti-sense technologies of developmental biology (*31–36*). Furthermore, a homopyrimidine TFO with MOR linkages binds with target duplex DNA to form stable triplex at neutral pH even in the absence of magnesium ion (*26*, *27*). The thermal stability of the triplex with MOR-modified TFO at neutral pH without magnesium ion was much higher than that with the corresponding natural phosphodiester TFO (*26*, *27*), which was shown by UV melting to analyse the dissociation process of the triplex. However, the formation process of the triplex involving MOR-modified TFO has not been well characterized yet. To explore the possibility for the application of MOR-modified TFO to the triplex formation-based anti-gene technologies as well as the widely used anti-sense technologies, the investigation of the formation process of the triplex involving MOR-modified TFO may be more important than that of the dissociation process of the same triplex. In addition, the mechanistic explanation for the MOR modification-mediated triplex stabilization at neutral pH without magnesium ion remains to be elucidated. In the present study, therefore, we have examined the thermodynamic and kinetic effects of the MOR modification of TFO on pyrimidine motif triplex formation at neutral pH without magnesium ion. The thermodynamic and kinetic effects of the MOR modification on the pyrimidine motif triplex formation between a 23-bp homopurine–homopyrimidine target duplex (Pur23A•Pyr23T) (Fig. 1b) and its specific 15-mer homopyrimidine unmodified TFO (Pyr15T) (Fig. 1b) or MOR-modified TFO (Pyr15MOR) (Fig. 1b) have been analysed by electrophoretic mobility shift assay (EMSA) (*37–40*), UV melting, isothermal titration calorimetry (ITC) (*38*, *39*, *41–44*), and interaction analysis system (IAsys) (*38–40*, *44–46*). We have found that the MOR modification of TFO increased the binding constant for the pyrimidine motif triplex formation at neutral pH without magnesium ion by more than 40-fold. Kinetic data have also demonstrated that the major contribution for the increase in the binding constant by the MOR modification resulted from the considerable increase in the association rate constant rather than the decrease in the dissociation rate constant. The ability of the MOR modification to promote pyrimidine motif triplex formation at neutral pH without magnesium ion would support further progress in therapeutic applications of the anti-gene strategy *in vivo*. The mechanism of the MOR modification to promote pyrimidine motif triplex formation will be discussed.

MATERIALS AND METHODS

Preparation of Oligonucleotides—We synthesized 23-mer complementary oligonucleotides for a target duplex, Pur23A and Pyr23T (Fig. 1b), a 15-mer homopyrimidine unmodified TFO specific for the target duplex, Pyr15T (Fig. 1b) and a 15-mer non-specific homopyrimidine oligonucleotide, Pyr15NS (Fig. 1b), on an ABI DNA synthesizer using the solid-phase cyanoethyl phosphoramidite method, and purified them with a reverse-phase high-performance liquid chromatography (HPLC) on a Wakosil DNA column. A 15-mer homopyrimidine MOR-modified TFO specific for the target duplex, Pyr15MOR (Fig. 1b), was purchased from Gene Tools Inc. 5′-Biotinylated Pyr23T (denoted as Bt-Pyr23T) was prepared using biotin phosphoramidite. The concentration of all oligonucleotides was determined by UV absorbance. Complementary strands, Pur23A and Pyr23T, were annealed by heating at up to 90°C, followed by a gradual cooling to room temperature. The annealed sample was applied on a hydroxyapatite column (BIORAD Inc.) to remove unpaired single strands. The concentration of the duplex DNA (Pur23A•Pyr23T) was determined by UV absorption considering the DNA concentration ratio of 1OD = 50 μg/ml, with a M_r of 15,180.

EMSA—EMSA experiments were performed essentially as described previously by a 15% native polyacrylamide gel electrophoresis (*38–40*).

DNase I Footprinting—Fluorescence IRD800-labelled Pur23A•Pyr23T duplex was mixed with a series of concentrations of the specific TFO (Pyr15T or Pyr15MOR) in buffer A (10 mM sodium cacodylate-cacodylic acid at pH 6.8 containing 200 mM NaCl). The final TFO

concentrations varied between 6.25–1600 μM for Pyr15T and 0.1–25 μM for Pyr15MOR. The mixtures (10 μl) were equilibrated at 4°C for 12 h. DNase I digestion was carried out by adding 10 U of DNase I (Toyobo) (1 μl) at room temperature. The reaction was stopped after 15 min by adding 15 μl of 20 mM EDTA and 90% formamide. The products of digestion were heated at 95°C for 5 min, cooled rapidly to 4°C, and then separated on a 15% denaturing polyacrylamide gel containing 7 M urea.

pH Stability Curves by UV Spectroscopy—pH stability curves experiments were performed on a DU-640 spectrophotometer (Beckman Inc.). Cell path length was 1 cm. The UV absorbance of the mixture containing 1 μM target duplex (Pur23A•Pyr23T) and 1 μM specific TFO (Pyr15T or Pyr15MOR) was measured at room temperature in 50 mM Tris–acetate (pH 5.1, 5.4, 5.7, 6.0, 6.3, 6.6 or 6.9) or 50 mM Tris–HCl (pH 7.2, 7.5, 7.8, 8.1, 8.4, 8.7 or 9.0) containing 100 mM NaCl with detection at 260 nm.

UV Melting—UV melting experiments were carried out on a DU-640 spectrophotometer (Beckman Inc.) equipped with a Peltier type cell holder. Cell path length was 1 cm. UV melting profiles were measured in buffer A (10 mM sodium cacodylate-cacodylic acid at pH 6.8 containing 200 mM NaCl) or buffer B (10 mM sodium cacodylate-cacodylic acid at pH 5.3 containing 200 mM NaCl) at a scan rate of 0.5°C/min with detection at 260 nm. The first derivative was calculated from the UV melting profile. The peak temperatures in the derivative curve were designated as the melting temperature, T_m. The triplex nucleic acid concentration used was 1 μM.

CD spectroscopy—CD spectra at 20°C were recorded in buffer A or buffer B on a JASCO J-720 spectropolarimeter interfaced with a microcomputer. Cell path length was 1 cm. The concentration of the triplex with the specific TFO (Pyr15T or Pyr15MOR), the target duplex (Pur23A•Pyr23T) and the specific TFO (Pyr15T or Pyr15MOR) used was 1 μM.

Isothermal Titration Calorimetry (ITC)—Isothermal titration experiments were carried out on a VP ITC system (Microcal Inc., USA), essentially as described previously (*38*, *39*, *44*). The TFO and Pur23A•Pyr23T duplex solutions were prepared by extensive dialysis against buffer A or buffer B. The TFO solution in buffer A or buffer B was injected in 5 μl increments and 10-min intervals into the Pur23A•Pyr23T duplex solution without changing the reaction conditions. The heat for each injection was subtracted by the heat of dilution of the injectant, which was measured by injecting the TFO solution into the same buffer. Each corrected heat was divided by the moles of the TFO solution injected, and analysed with Microcal Origin software supplied by the manufacturer.

Interaction Analysis System (IAsys)—Kinetic experiments by resonant mirror method were performed on an IAsys Plus instrument (Affinity Sensors Cambridge Inc., UK), essentially as described previously, where a real-time biomolecular interaction was measured with a laser biosensor (*38–40*, *44*).

RESULTS

EMSA of Pyrimidine Motif Triplex Formation at neutral pH—The pyrimidine motif triplex formation of the target duplex (Pur23A•Pyr23T; Fig. 1b) with its specific unmodified (Pyr15T; Fig. 1b) or MOR-modified (Pyr15MOR; Fig. 1b) TFO was examined at pH 7.0 without magnesium ion by EMSA (Fig. 2). Total oligonucleotide concentration [specific TFO (Pyr15T or Pyr15MOR; Fig. 1b)] + [non-specific oligonucleotide (Pyr15NS; Fig. 1b)]) was kept constant at 10 μM to minimize loss of DNA during processing and to assess sequence specificity. While incubation with 10 μM Pyr15NS alone did not cause a shift in electrophoretic migration of the target duplex (see lane 1 for each condition), those with Pyr15T or Pyr15MOR at particular concentrations caused retardation of the duplex migration owing to triplex formation (*37*). The dissociation constant, K_d, of triplex formation was determined from the concentration of the TFO, which caused half of the target duplex to shift to the triplex (*37*). The K_d of the triplex with Pyr15T was estimated to be ~10 μM. In contrast, the K_d of the triplex with Pyr15MOR was ~0.2 μM, indicating that the MOR modification of TFO increased the binding affinity of the pyrimidine motif triplex formation at neutral pH without magnesium ion by ~50-fold.

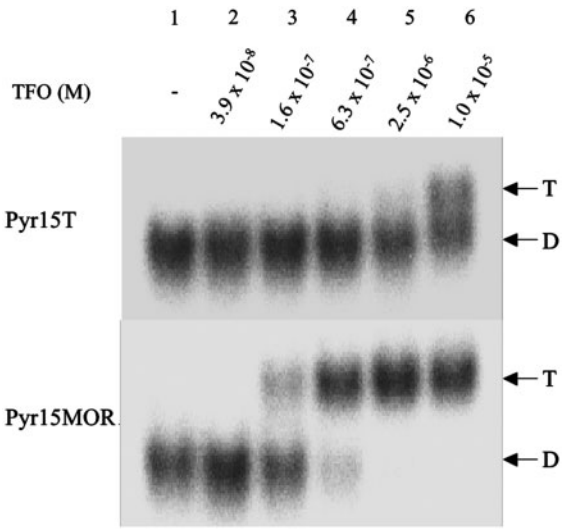

Fig. 2. **EMSA of the pyrimidine motif triplex formation with the specific TFO (Pyr15T or Pyr15MOR) at neutral pH.** Triplex formation was initiated by adding ^{32}P-labeled Pur23A•Pyr23T duplex (0.1 pmol) with the indicated final concentrations of the specific TFO (Pyr15T or Pyr15MOR). The non-specific TFO (Pyr15NS) was added to adjust the equimolar concentrations (10 μM) of TFO (Pyr15T + Pyr15NS or Pyr15MOR + Pyr15NS) in each lane. Reaction mixtures involving Pyr15T or Pyr15MOR in buffer [50 mM Tris–acetate (pH 7.0) and 100 mM sodium chloride] were incubated for 6 h at 37°C, and then electrophoretically separated on a 15% native polyacrylamide gel at 4°C. Positions of the duplex (D) and triplex (T) are indicated.

DNaseI Footprinting of Pyrimidine Motif Triplex Formation at Neutral pH—The binding affinity and selectivity of the pyrimidine motif triplex formation with unmodified (Pyr15T) or MOR-modified (Pyr15MOR) TFO, and the structures of the formed triplex were assessed at pH 6.8 without magnesium ion by DNase I footprinting (Fig. 3). Non-specific oligonucleotide

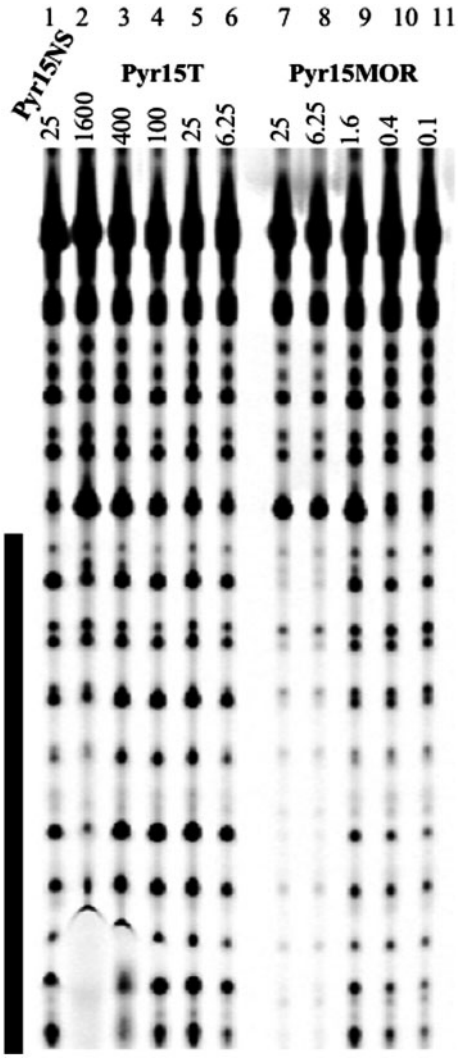

Fig. 3. **DNase I footprinting experiments for the interaction of the non-specific oligonucleotide (Pyr15NS) (lane 1) or the specific TFO [Pyr15T (lanes 2–6) and Pyr15MOR (lanes 7–11)] with the target duplex DNA fragment (Pur23A•Pyr23T).** The filled box shows the position of the target site. The oligonucleotide or TFO concentration (μM) is shown at the top of each gel lane. The triplex formation was performed in buffer A at pH 6.8 (see MATERIALS AND METHODS section). The mixtures were equilibrated at 4°C for 12 h before DNase I digestion.

(Pyr15NS) at the concentration of 25 μM shows no interaction with the target site (lane 1). Although no footprints are observed for Pyr15T at the concentrations of 25 μM (lane 5) and 6.25 μM (lane 6), clear footprints are evident for Pyr15MOR at the same concentrations [25 μM (lane 7) and 6.25 μM (lane 8)]. Even at the concentration as high as 1600 μM (lane 2), Pyr15T produces no evident footprints. These results indicate that the MOR modification of TFO increased the binding affinity of the pyrimidine motif triplex formation at neutral pH, consistent with the results of EMSA (Fig. 2).

Spectroscopic Characterization of Pyrimidine Motif Triplex—To examine the pH effect on the pyrimidine

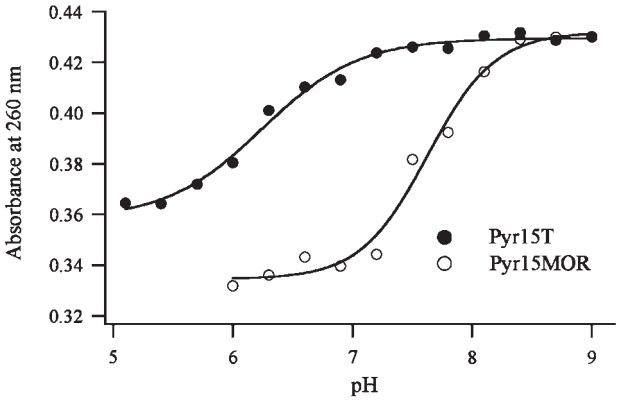

Fig. 4. **pH stability curves for the mixture containing the target duplex (Pur23A•Pyr23T) and the specific TFO (Pyr15T or Pyr15MOR).** The UV absorbance of the mixture containing 1 μM Pur23A•Pyr23T and 1 μM Pyr15T or Pyr15MOR was measured at room temperature in 50 mM Tris–acetate (pH 5.1, 5.4, 5.7, 6.0, 6.3, 6.6, or 6.9) or 50 mM Tris–HCl (pH 7.2, 7.5, 7.8, 8.1, 8.4, 8.7, or 9.0) containing 100 mM NaCl with detection at 260 nm. Cell path length was 1 cm.

motif triplex formation, we have determined pH stability curves for the pyrimidine motif triplex with unmodified (Pyr15T) or MOR-modified (Pyr15MOR) TFO at room temperature. The UV absorbance (260 nm) of the mixture containing the target duplex (Pur23A•Pyr23T) and the specific TFO (Pyr15T or Pyr15MOR) was measured at room temperature as a function of pH without magnesium ion (Fig. 4). For the pH values higher than 7.2 for Pyr15T and for those higher than 8.4 for Pyr15MOR, the UV absorbance of the mixture did not change significantly. When the pH value of the mixture was below 7.2 for Pyr15T and below 8.4 for Pyr15MOR, a hypochromic effect was observed because the TFO (Pyr15T or Pyr15MOR) was able to bind with the major groove of the target duplex (Pur23A•Pyr23T) to form the triplex. The pH-induced transition of the UV absorbance (260 nm) results from protonation at N3 of cytosines in the TFO (Pyr15T or Pyr15MOR) to form Hoogsteen hydrogen bonds with the Watson–Crick G:C base pairs of the target duplex (Pur23A•Pyr23T). The pH stability curve for Pyr15MOR was shifted to basic pH in comparison with that for Pyr15T, indicating that the triplex with Pyr15MOR at neutral pH was more stable than that with Pyr15T, consistent with the results of EMSA (Fig. 2) and DNase I footprinting (Fig. 3). From the pH stability curves, we have found that cytosines of Pyr15MOR are almost fully protonated in the triplex at pH 6.8. Hoogsteen hydrogen bonds as to C^+•G:C are formed just as to T•A:T in the triplex with Pyr15MOR at pH 6.8.

The thermal stability of the pyrimidine motif triplex with unmodified (Pyr15T) or MOR-modified (Pyr15MOR) TFO was investigated at pH 6.8 without magnesium ion by UV melting (Fig. 5). To investigate the pH dependence of the thermal stability of the pyrimidine motif triplex, the UV melting analyses of the pyrimidine motif triplex with Pyr15T was also performed

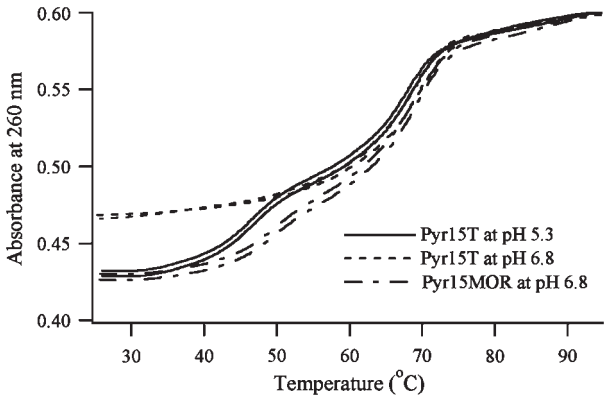

Fig. 5. **UV-melting profiles of the pyrimidine motif triplex with the specific TFO (Pyr15T or Pyr15MOR) in both directions (heating and cooling).** The triplex with Pyr15T or Pyr15MOR in buffer A at pH 6.8 (see MATERIALS AND METHODS section) and with Pyr15T in buffer B at pH 5.3 (see MATERIALS AND METHODS section) were melted at a scan rate of 0.5°C/min with detection at 260 nm. Cell path length was 1 cm. The triplex nucleic acid concentration used was 1 μM.

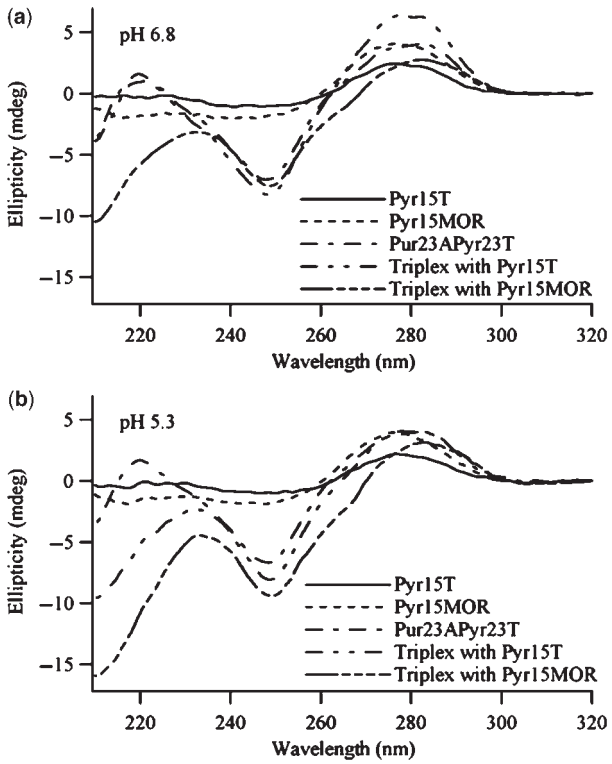

Fig. 6. **CD spectra of the pyrimidine motif triplex involving the specific TFO (Pyr15T or Pyr15MOR), the target duplex (Pur23A•Pyr23T) and the specific TFO (Pyr15T or Pyr15MOR) at pH 6.8 (a) and pH 5.3 (b).** The triplex with the specific TFO (Pyr15T or Pyr15MOR), the target duplex (Pur23A•Pyr23T) and the specific TFO (Pyr15T or Pyr15MOR) in buffer A at pH 6.8 (see MATERIALS AND METHODS section) (a) and in buffer B at pH 5.3 (see MATERIALS AND METHODS section) (b) were measured at 20°C in the wavelength range of 210–320 nm. Cell path length was 1 cm. The concentration of the triplex, the target duplex and the specific TFO used was 1 μM.

at pH 5.3 without magnesium ion. UV melting curves in the both directions (heating and cooling) are almost superimposable in all cases, indicating that the dissociation and association processes are reversible. The triplex with Pyr15MOR at pH 6.8 and that with Pyr15T at pH 5.3 showed two-step melting. The first transition at lower temperature, T_{m1} (49.9°C for Pyr15MOR at pH 6.8 and 47.1°C for Pyr15T at pH 5.3), was the melting of the triplex to a duplex and a TFO, and the second transition at higher temperature, T_{m2} (69.5°C for Pyr15MOR at pH 6.8 and 68.5°C for Pyr15T at pH 5.3), was the melting of the duplex. On the other hand, only one transition at higher temperature, $T_m = 69.8$°C was observed for Pyr15T at pH 6.8. As the values of T_{m2} for Pyr15T at pH 5.3 and T_m for Pyr15T at pH 6.8 were almost similar, and the magnitude in UV absorbance change at T_m for Pyr15T at pH 6.8 was almost equal to that at T_{m2} for Pyr15T at pH 5.3, the transition at T_m for Pyr15T at pH 6.8 was identified as the melting of the duplex, indicating no stable triplex with Pyr15T at pH 6.8. These results demonstrate that the thermal stability of the triplex with Pyr15MOR at pH 6.8 was significantly higher than that with Pyr15T at pH 6.8, confirming, like others (*26*, *27*), that the MOR modification of TFO increased the thermal stability of the pyrimidine motif triplex at neutral pH without magnesium ion.

To further characterize the triplexes involving Pyr15T or Pyr15MOR, CD spectra of the triplex with the specific TFO (Pyr15T or Pyr15MOR), the target duplex (Pur23A•Pyr23T) and the specific TFO (Pyr15T or Pyr15MOR) were measured at pH 6.8 and pH 5.3 without magnesium ion (Fig. 6). A significant negative band in the short-wavelength (210–220 nm) region of the CD profile was observed for the triplex with Pyr15MOR at pH 6.8 and for that with each of Pyr15T and Pyr15MOR at pH 5.3 (Fig. 6). The significant negative band was not observed for the target duplex (Pur23A•Pyr23T) and the specific TFO (Pyr15T or Pyr15MOR (Fig. 6). As the significant negative band has been considered as the trademark for the pyrimidine motif triplex (*47*), the observed spectra confirms the triplex formation involving Pyr15MOR at pH 6.8 and that involving each of Pyr15T and Pyr15MOR at pH 5.3. The overall shape of the CD spectra was quite similar among these profiles, suggesting that no significant change may be induced in the higher-order structure of the pyrimidine motif triplex by the MOR modification. On the other hand, no significant negative band in the short-wavelength (210–220 nm) region of the CD profile was observed for the triplex with Pyr15T at pH 6.8, and the CD spectrum pattern for the triplex with Pyr15T at pH 6.8 is almost superimposable to that for the target duplex [Pur23A•Pyr23T (Fig. 6)], indicating no stable triplex formation for Pyr15T at pH 6.8, consistent with the results of UV melting (Fig. 5).

Thermodynamic Analyses of Pyrimidine Motif Triplex Formation by ITC—We examined the thermodynamic parameters of the pyrimidine motif triplex formation between a 23-bp target duplex (Pur23A•Pyr23T) and each of its specific 15-mer unmodified (Pyr15T) and

MOR-modified (Pyr15MOR) TFO at 25°C and pH 6.8 without magnesium ion by ITC. To investigate the pH dependence of the pyrimidine motif triplex formation, the thermodynamic parameters of the triplex formation between Pur23A•Pyr23T and each of Pyr15T and Pyr15MOR were also analysed at 25°C and pH 5.3 without magnesium ion by ITC. Figure 7a shows a typical ITC profile for the triplex formation between Pyr15MOR and Pur23A•Pyr23T at 25°C and pH 6.8. An exothermic heat pulse was observed after each injection of Pyr15MOR into Pur23A•Pyr23T. The magnitude of each peak decreased gradually with each new injection, and a small peak was still observed at a molar ratio of [Pyr15MOR]/[Pur23A•Pyr23T] = 2. The area of the small peak was equal to the heat of dilution measured in a separate experiment by injecting Pyr15MOR into the same buffer. The area under each peak was integrated, and the heat of dilution of Pyr15MOR was subtracted from the integrated values. The corrected heat was divided by the moles of injected solution, and the resulting values were plotted as a function of a molar ratio of [Pyr15MOR]/[Pur23A•Pyr23T], as shown in Fig. 7b. The resultant titration plot was fitted to a sigmoidal curve by a non-linear least-squares method. The binding constant, K_a, and the enthalpy change, ΔH, were obtained from the fitted curve (*43*). The Gibbs free energy change, ΔG, and the entropy change, ΔS, were calculated from the equation, $\Delta G = -RT\ln K_a = \Delta H - T\Delta S$, where R is gas constant and T is temperature (*43*). The titration plots for Pyr15T at pH 5.3 and for Pyr15MOR at pH 5.3 are also shown in Fig. 7b. The thermodynamic parameters for Pyr15T at pH 5.3 and for Pyr15MOR at pH 5.3 were obtained from the titration plot in the same way. On the other hand, we were unable to obtain a sigmoidal titration plot and the thermodynamic parameters for Pyr15T at pH 6.8, because the K_a for Pyr15T at pH 6.8 was below the lowest detection limit of ITC measurement (*43*). The significantly lower K_a for Pyr15T at pH 6.8 in comparison with that for Pyr15MOR at pH 6.8 indicates that the MOR modification of TFO increases the K_a for the pyrimidine motif triplex formation at neutral pH without magnesium ion, which is consistent with the results of EMSA (Fig. 2) and DNaseI footprinting (Fig. 3). In addition, the significantly lower K_a for Pyr15T at pH 6.8 in comparison with that for Pyr15T at pH 5.3 confirms, similar to others (*6–8*), that neutral pH is unfavourable for the pyrimidine motif triplex formation involving C^+•G:C triads.

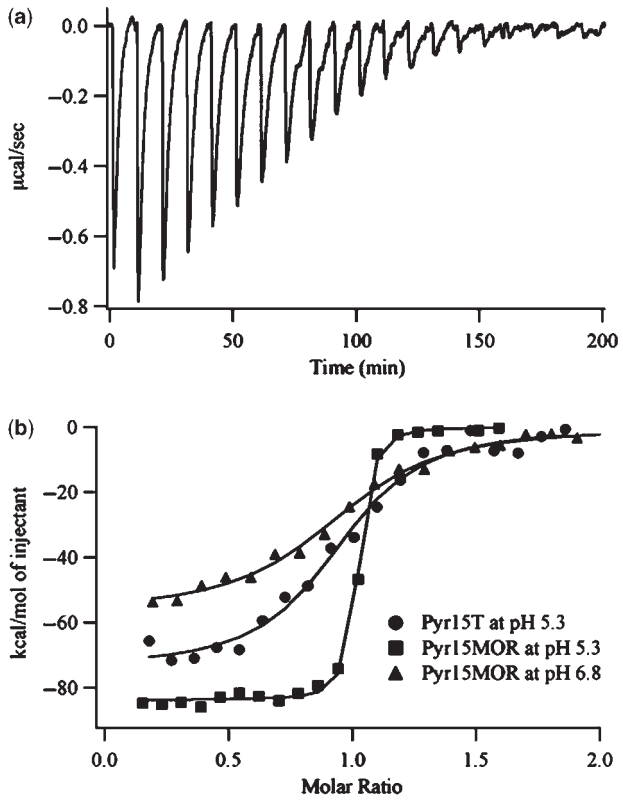

Fig. 7. **Thermodynamic analyses of the pyrimidine motif triplex formation with Pyr15MOR at pH 6.8 and pH 5.3 and with Pyr15T at pH 5.3 by ITC.** (a) Typical ITC profiles for the triplex formation between Pyr15MOR and Pur23A•Pyr23T at 25°C and pH 6.8. Pyr15MOR solution measuring 460 µM in buffer A (see MATERIALS AND METHODS section) was injected 20 times in 5 µl increments into 16.6 µM Pur23A•Pyr23T solution, which was dialysed against the same buffer. Injections were occurred over 12 s at 10-min intervals. (b) The titration plots against the molar ratio of [TFO]/[Pur23A•Pyr23T]. The data were fitted by a non-linear least-squares method.

Table 1 summarizes the thermodynamic parameters for the pyrimidine motif triplex formation with Pyr15MOR at 25°C and pH 6.8, and those with each of Pyr15T and Pyr15MOR at 25°C and pH 5.3, obtained from ITC. The signs of both ΔH and ΔS were negative under each condition. As an observed negative ΔS was unfavourable for the triplex formation, the triplex formation was driven by a large negative ΔH under each condition. Although the K_a and ΔG for the triplex formations with Pyr15MOR at pH 6.8 and with Pyr15T at pH 5.3 are quite similar, the ingredients of ΔG, that is, ΔH and ΔS, are obviously different from each other (Table 1). The magnitudes of the negative ΔH and ΔS for Pyr15MOR at pH 6.8 are significantly smaller than those observed for Pyr15T at pH 5.3 (Table 1). On the

Table 1. **Thermodynamic parameters for the pyrimidine motif triplex formation with Pyr15T or Pyr15MOR at 25°C, obtained from ITC.**

TFO	pH	K_a (M^{-1})	ΔG (kcal mol^{-1})	ΔH (kcal mol^{-1})	ΔS (cal mol^{-1} K^{-1})
Pyr15T	5.3[a]	$(2.82 \pm 0.65) \times 10^6$	-8.80 ± 0.15	-73.9 ± 2.3	-218 ± 8
Pyr15T	6.8[b]	N.D.[c]	N.D.[c]	N.D.[c]	N.D.[c]
Pyr15MOR	5.3[a]	$(9.27 \pm 1.55) \times 10^7$	-10.87 ± 0.11	-83.1 ± 0.5	-242 ± 2
Pyr15MOR	6.8[b]	$(1.01 \pm 0.16) \times 10^6$	-8.19 ± 0.10	-55.2 ± 1.6	-158 ± 6

[a]10 mM sodium cacodylate-cacodylic acid (pH 5.3) and 200 mM sodium chloride. [b]10 mM sodium cacodylate-cacodylic acid (pH 6.8) and 200 mM sodium chloride. [c]Not determined.

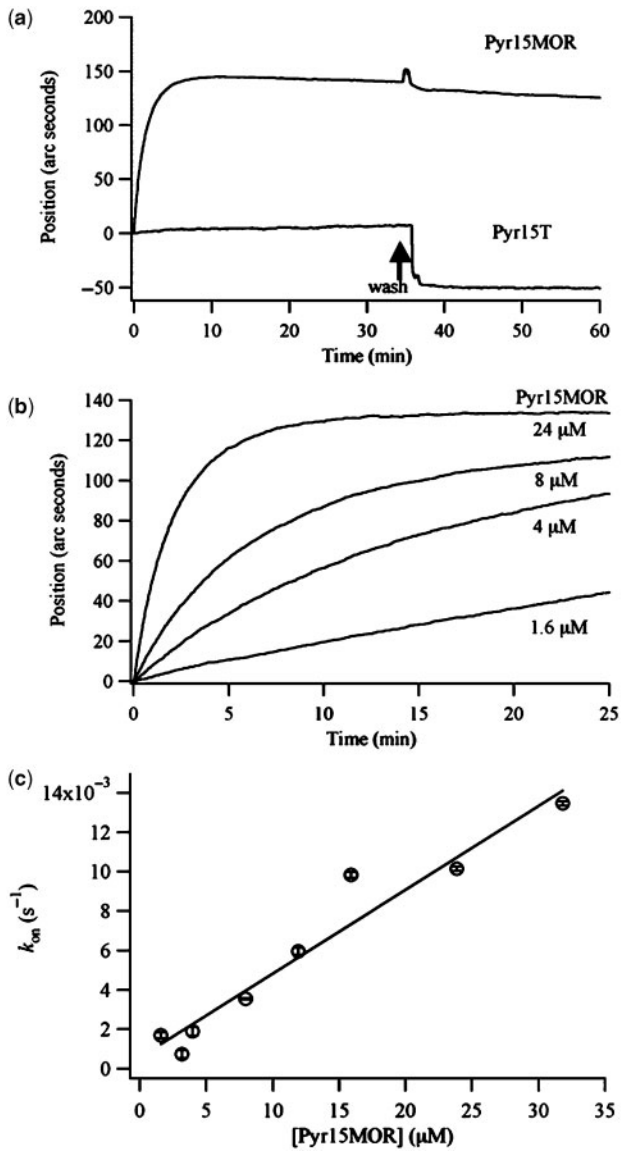

Fig. 8. **Kinetic analyses of the pyrimidine motif triplex formation with the specific TFO (Pyr15T or Pyr15MOR) at pH 6.8 by IAsys.** (a) Typical IAsys sensorgrams for the triplex formation at 25°C and pH 6.8 after injecting 32 μM specific TFO (Pyr15T or Pyr15MOR) into the Bt-Pyr23T•Pur23A-immobilized cuvette are shown. (b) A series of sensorgrams for the triplex formation between Pyr15MOR and Pur23A•Pyr23T at 25°C and pH 6.8. The Pyr15MOR solution, diluted in buffer A (see MATERIALS AND METHODS section) to achieve the indicated final concentration, was injected into the Bt-Pyr23T•Pur23A-immobilized cuvette. The binding of Pyr15MOR to Bt-Pyr23T•Pur23A was monitored as the response against time. (c) Measured on-rate constants, k_{on}, of the triplex formation in (b) were plotted against the respective concentrations of Pyr15MOR. The plot was fitted to a straight line ($r^2 = 0.97$) by a linear least-squares method.

other hand, although the magnitudes of K_a, the negative ΔG, and the negative ΔH for the triplex formation with Pyr15MOR at pH 5.3 are significantly larger than those observed for the triplex formation with Pyr15T at pH 5.3, the magnitudes of the negative ΔS for the triplex formations with Pyr15MOR at pH 5.3 and with Pyr15T at pH 5.3 are similar.

Kinetic Analyses of Pyrimidine Motif Triplex Formation at Neutral pH by IAsys—To examine the putative mechanism involved in the increase in K_a for the pyrimidine motif triplex formation by the MOR modification (Figs 2 and 3, and Table 1), we assessed the kinetic parameters for the association and dissociation of TFO (Pyr15T or Pyr15MOR) with Pur23A•Pyr23T at 25°C and pH 6.8 without magnesium ion by IAsys. Figure 8a compares the sensorgrams representing the triplex formation and dissociation involving 32 μM of the specific TFO (Pyr15T or Pyr15MOR). The injection of Pyr15T over the immobilized Bt-Pyr23T•Pur23A duplex caused an increase in response. The change in the association curve with time for Pyr15MOR was substantially enhanced than that for Pyr15T, although the change in the dissociation curve for Pyr15MOR was almost similar to that for Pyr15T. The results indicate that the MOR modification of TFO remarkably increases the association rate constant of the triplex equilibrium.

To understand the kinetic parameters more quantitatively, we analysed a series of association and dissociation curves at the various concentrations of TFO. As shown in Fig. 8b, an increase in the concentration of Pyr15MOR led to a gradual change in the response of the association curves. The on-rate constant (k_{on}) was obtained from the analysis of each association curve. Figure 8c shows a plot of k_{on} against the Pyr15MOR concentrations. The resultant plot was fitted to a straight line by a linear least-squares method. The association rate constant (k_{assoc}) was determined from the slope of the fitted line (*45*, *46*). The off-rate constant (k_{off}) was obtained from the analysis of each dissociation curve (Fig. 8a and data not shown). As k_{off} is usually independent of the concentration of the injected solution, the dissociation rate constant (k_{dissoc}) was determined by averaging k_{off} for several concentrations (*45*, *46*). K_a was calculated from the equation, $K_a = k_{assoc}/k_{dissoc}$. The kinetic parameters for Pyr15T were obtained in the same way.

Table 2 summarizes the kinetic parameters for the pyrimidine motif triplex formation with Pyr15T or Pyr15MOR at 25°C and pH 6.8, obtained from IAsys. The K_a for Pyr15MOR at pH 6.8 was ~50-fold larger than that observed for Pyr15T at pH 6.8, indicating that the MOR modification of TFO increased the K_a for the pyrimidine motif triplex formation at neutral pH without magnesium ion, which supported the results of EMSA (Fig. 2), DNase I footprinting (Fig. 3) and ITC (Table 1). The MOR modification of TFO increased k_{assoc} by ~26-fold, while decreasing k_{dissoc} by only 1.8-fold. Thus, the much larger K_a by the MOR modification of TFO resulted mainly from the increase in k_{assoc} rather than the decrease in k_{dissoc}.

DISCUSSION

The K_a for the pyrimidine motif triplex formation with Pyr15T at pH 5.3 was significantly larger than that observed with Pyr15T at pH 6.8 (Table 1). The thermal

Table 2. **Kinetic parameters of the pyrimidine motif triplex formation with Pyr15T or Pyr15MOR at 25°C and pH 6.8 in 10 mM sodium cacodylate-cacodylic acid and 200 mM sodium chloride, obtained from IAsys surface affinity assay.**

TFO	k_{assoc} ($M^{-1}s^{-1}$)	k_{assoc} (relative)	k_{dissoc} (s^{-1})	k_{dissoc} (relative)	K_a (M^{-1})	K_a (relative)
Pyr15T	$(1.63 \pm 0.09) \times 10$	1.0	$(4.19 \pm 0.83) \times 10^{-3}$	1.0	$(3.89 \pm 1.23) \times 10^{3}$	1.0
Pyr15MOR	$(4.25 \pm 0.41) \times 10^{2}$	26.1	$(2.35 \pm 1.32) \times 10^{-3}$	0.56	$(1.81 \pm 0.17) \times 10^{5}$	46.5

stability of the pyrimidine motif triplex with Pyr15T at pH 5.3 was substantially higher than that observed with Pyr15T at pH 6.8 (Fig. 5). These results are consistent with the previously reported results that neutral pH is unfavourable for the pyrimidine motif triplex formation involving C^+•G:C triads (*6–8*). On the other hand, the K_a for the pyrimidine motif triplex formation with Pyr15MOR at pH 6.8 was ~50-fold larger than that observed with Pyr15T at pH 6.8 (Table 2). The increase in K_a at neutral pH by the MOR modification of TFO was supported by the results of EMSA (Fig. 2), DNaseI footprinting (Fig. 3) and ITC (Table 1). In addition, the MOR modification of TFO increased the thermal stability of the pyrimidine motif triplex at neutral pH (Fig. 5), which confirms the results obtained by other groups (*26*, *27*). These results indicate that the MOR modification of TFO promotes the pyrimidine motif triplex formation at neutral pH.

The pH stability curve for Pyr15MOR was shifted to basic pH in comparison with that for Pyr15T (Fig. 4), indicating that the triplex with Pyr15MOR at neutral pH was more stable than that with Pyr15T, consistent with the results of EMSA (Fig. 2), DNase I footprinting (Fig. 3) and ITC (Table 1). From the pH stability curves, we have found that cytosines of Pyr15MOR are almost fully protonated in the triplex at pH 6.8. Hoogsteen hydrogen bonds as to C^+•G:C are formed just as to T•A:T in the triplex with Pyr15MOR at pH 6.8. Because the MOR modification does not include base modification, it is unlikely that protonation/deprotonation pK_a of cytosine bases of the free MOR-modified TFO (Pyr15MOR) is shifted by the MOR modification itself. The MOR modification of TFO may promote the assembly of the TFO (Pyr15MOR) and the target duplex (Pur23A•Pyr23T), which may enhance protonation of cytosine bases of Pyr15MOR to form the triplex. Thus, the pK_a shift of cytosine bases of Pyr15MOR in the triplex may be caused by the intrinsic stability of the triplex with Pyr15MOR.

The K_a and ΔG for the pyrimidine motif triplex formations with Pyr15MOR at pH 6.8 and with Pyr15T at pH 5.3 were quite similar (Table 1). However, the ingredients of ΔG, that is, ΔH and ΔS, were obviously different from each other. The magnitudes of the negative ΔH and ΔS for Pyr15MOR at pH 6.8 were significantly smaller than those observed for Pyr15T at pH 5.3 (Table 1). The negative ΔH upon the triplex formation measured by ITC reflects a major contribution from the hydrogen bonding and the base stacking involved in the triplex formation (*48–51*). The immobilization of electrostricted water molecules around polar atoms upon the triplex formation is also considered to be the major sources of the negative ΔH upon the triplex formation (*48–51*). Thus, the difference in ΔH for the triplex formations between Pyr15MOR at pH 6.8 and Pyr15T at pH 5.3 suggests that the hydrogen bonding and/or the base stacking of the triplex with the MOR-modified TFO and the degree of the immobilization of water molecules around the protonated cytosine bases and polar nitrogen atoms of the triplex with the MOR-modified TFO may be significantly different from those with the corresponding unmodified TFO. It is likely that the degree of the hydrogen bonding and the base stacking may be changed by the MOR modification, which is undetectable by CD (Fig. 6). Further analyses are necessary to understand the precise reason for the difference in ΔH. On the other hand, the negative ΔS upon the triplex formation measured by ITC is mainly contributed by a negative conformational entropy change due to the conformational restraint of TFO involved in the triplex formation (*48–51*). Therefore, the smaller magnitude of the negative ΔS for Pyr15MOR at pH 6.8 in comparison with that for Pyr15T at pH 5.3 (Table 1) suggests that the MOR-modified TFO in the free state may be more rigid than the corresponding unmodified TFO. The increased rigidity of the MOR-modified TFO in the free state relative to the corresponding unmodified TFO causes the smaller entropic loss upon the triplex formation with the MOR-modified TFO at neutral pH, which provides a favourable component to the ΔG and leads to the increase in the K_a for the triplex formation at neutral pH. We conclude that the increased rigidity of the MOR-modified TFO in the free state may be one of the important factors to increase the K_a for the pyrimidine motif triplex formation.

The magnitudes of K_a and the negative ΔG for Pyr15MOR at pH 5.3 were significantly larger than those for Pyr15T at pH 5.3. When the ΔG is calculated from the fitting procedure of ITC, the energy observed by ITC is divided not by the effective concentration really involved in the triplex formation but by the apparent concentration added to the triplex formation. The calculation does not take it into consideration what percentage of the added concentration is really effectively involved in the triplex formation. Thus, if the triplex formation is less stoichiometric under a certain condition, the magnitude of ΔG for the less stoichiometric triplex formation estimated by ITC is smaller than that observed for the more stoichiometric triplex formation under another condition. Therefore, the significantly smaller magnitude of ΔG for Pyr15T at pH 5.3 relative to that for Pyr15MOR at pH 5.3 (Table 1) suggests that the triplex formation with Pyr15T at pH 5.3 was significantly less stoichiometric than that with Pyr15MOR at pH 5.3. On the other hand, unlike the significantly different ΔG between Pyr15T at pH 5.3 and Pyr15MOR at pH 5.3, the magnitude of the negative ΔS for Pyr15MOR at pH 5.3 was apparently similar to that observed for Pyr15T at pH 5.3. However, the amount of the really formed

triplex with Pyr15MOR at pH 5.3 may be significantly larger than that with Pyr15T at pH 5.3, because the triplex formation with Pyr15MOR at pH 5.3 was more stoichiometric as discussed above. Thus, the magnitude of the negative ΔS for the really occurred triplex formation with Pyr15MOR at pH 5.3 may be significantly smaller than that with Pyr15T at pH 5.3. The negative ΔS upon the triplex formation is mainly contributed by a negative conformational entropy change due to the conformational restraint of TFO involved in the triplex formation. Therefore, the smaller magnitude of the negative ΔS for the really occurred triplex formation with Pyr15MOR at pH 5.3 relative to that with Pyr15T at pH 5.3 suggests that the MOR-modified TFO in the free state is more rigid than the corresponding unmodified TFO. The more rigidity of the MOR-modified TFO in the free state relative to the corresponding unmodified TFO causes the smaller entropic loss upon the really occurred triplex formation with the MOR-modified TFO, which provides a favourable component to the ΔG and leads to the increase in the K_a of the triplex formation. On the basis of these considerations, we conclude that the more rigidity of the MOR-modified TFO in the free state may be one of the factors to increase the K_a for the pyrimidine motif triplex formation. The lone electron pair of the nitrogen atom of the morpholino ring may be delocalized to the non-briging oxygen atom of the phosphate group. The electronic conjugation may result in more rigidity of morpholino backbone relative to phosphodiester backbone.

Kinetic data have demonstrated that the MOR modification of TFO considerably increased the k_{assoc} of the pyrimidine motif triplex formation at neutral pH (Table 2). The increase in the k_{assoc} is a plausible kinetic reason to explain the remarkable gain in the K_a at neutral pH by the MOR modification (Figs 2 and 3, and Tables 1 and 2). Both our group (*50*) and others (*52*) have previously proposed a model that triplexes form along nucleation-elongation processes: in a nucleation step only a few base contacts of the Hoogsteen hydrogen bonds may be formed between TFO and the target duplex, and this may be followed by an elongation step, in which Hoogsteen base pairings progress to complete triplex formation. Both groups (*50*, *52*) have also suggested that the observed K_a, which is the ratio of k_{assoc} to k_{dissoc}, may mostly reflect a rapid equilibrium of the nucleation step, which is probably the rate-limiting process of the triplex formation. Electrostatic repulsion between TFO and the target duplex caused by excess accumulation of phosphate anions in the nucleation step may limit the rate of the triplex formation (*21*, *22*). The absence of negative charge in the MOR linkage may reduce the electrostatic repulsion between TFO and the target duplex, which may result in the acceleration of the nucleation step. Although low concentration (~0.8 mM) of magnesium ion was observed in the cell (*23*), most of *in vitro* triplex formation experiments were performed in the presence of high concentration (5–10 mM) of magnesium ion to reduce the electrostatic repulsion upon the triplex formation. In contrast, both the present study and other groups' previously reported results (*26*, *27*) showed that, even in the absence of magnesium ion, the MOR modification of TFO achieved the stable pyrimidine motif triplex at neutral pH, which may improve the therapeutic potential of the triplex. The acceleration of the nucleation step due to the reduction of the electrostatic repulsion between TFO and the target duplex by the non-charged MOR-modified TFO may enable the efficient pyrimidine motif triplex formation even in the absence of magnesium ion. Due to the more rigidity of morpholino backbone relative to phosphodiester backbone discussed above, the number of the possible conformations of the free MOR-modified TFO (Pyr15MOR) may be smaller than that of the free phosphodiester TFO (Pyr15T). Thus, it may take less time for Pyr15MOR to search for the competent nucleated state with the target duplex (Pur23A•Pyr23T), which has the ability to proceed to the elongation step. The shorter time to search for the competent nucleated state may result in larger k_{assoc} and resultant larger K_a for Pyr15MOR. Based on these considerations, we conclude that the MOR modification of TFO is considered to accelerate the nucleation step by reducing the electrostatic repulsion between TFO and the target duplex to increase the K_a for the pyrimidine motif triplex formation at neutral pH without magnesium ion.

Recently, MOR-modified oligonucleotides have been widely used as antisense agents to inhibit translation of target mRNA, especially in antisense technologies of developmental biology (*31–36*). The present study has clearly demonstrated that the MOR modification of TFO promotes the pyrimidine motif triplex formation at neutral pH without magnesium ion. Our results certainly support the idea that the MOR-modified oligonucleotides may have a potential to be applied to the triplex formation-based anti-gene technologies to inhibit transcription of target genes as well as the widely used anti-sense technologies. In addition, the present study has revealed that the more rigidity of the MOR-modified TFO in the free state may enable the significant increase in the K_a for the pyrimidine motif triplex formation at neutral pH without magnesium ion. The present study has also indicated that the significant increase in the K_a for the pyrimidine motif triplex formation at neutral pH without magnesium ion by the MOR modification of TFO mainly results from the considerable increase in the k_{assoc} probably by reducing the electrostatic repulsion between TFO and the target duplex. This information will present an effective approach for designing novel chemically modified TFO with higher binding affinity in the triplex formation under physiological conditions, which may eventually lead to progress in therapeutic applications of the anti-gene strategy *in vivo*.

ACKNOWLEDGEMENTS

We gratefully acknowledge Mr. Y. Tamura and Mr. K. Kawahashi for their helpful technical assistance in the initial stage of our study.

FUNDING

Grant-in-Aid from the Ministry of Education, Science, Sports, and Culture of Japan (17012022 and 17053027 to H.T.); Casio Science Promotion Foundation; Nakatani

Foundation of Electronic Measuring Technology Advancement; Iketani Science and Technology Foundation; and Kumagai Foundation for Science and Technology.

CONFLICT OF INTEREST

None declared.

REFERENCES

1. Chin, J.Y., Schleifman, E.B., and Glazer, P.M. (2007) Repair and recombination induced by triple helix DNA. *Front Biosci.* **12**, 4288–4297
2. Bissler, J.J. (2007) Triplex DNA and human disease. *Front Biosci.* **12**, 4536–4546
3. Duca, M., Vekhoff, P., Oussedik, K., Halby, L., and Arimondo, P.B. (2008) The triple helix: 50 years later, the outcome. *Nucleic Acids Res.* **36**, 5123–5138
4. Jain, A., Wang, G., and Vasquez, K.M. (2008) DNA triple helices: Biological consequences and therapeutic potential. *Biochimie* **90**, 1117–1130
5. Wells, R.D. (2008) DNA triplexes and Friedreich ataxia. *FASEB J.* **22**, 1625–1634
6. Frank-Kamenetskii, M.D. (1992) Protonated DNA structures. *Methods Enzymol.* **211**, 180–191
7. Singleton, S.F. and Dervan, P.B. (1992) Influence of pH on the equilibrium association constants for oligodeoxyribonucleotide-directed triple helix formation at single DNA sites. *Biochemistry* **31**, 10995–11003
8. Shindo, H., Torigoe, H., and Sarai, A. (1993) Thermodynamic and kinetic studies of DNA triplex formation of an oligohomopyrimidine and a matched duplex by filter binding assay. *Biochemistry* **32**, 8963–8969
9. Milligan, J.F., Krawczyk, S.H., Wadwani, S., and Matteucci, M.D. (1993) An anti-parallel triple helix motif with oligodeoxynucleotides containing 2′-deoxyguanosine and 7-deaza-2′-deoxyxanthosine. *Nucleic Acids Res.* **21**, 327–333
10. Cheng, A J. and Van Dyke, M.W. (1993) Monovalent cation effects on intermolecular purine-purine-pyrimidine triple-helix formation. *Nucleic Acids Res.* **21**, 5630–5635
11. Lee, J.S., Woodsworth, M.L., Latimer, L.J., and Morgan, A.R. (1984) Poly(pyrimidine). poly(purine) synthetic DNAs containing 5-methylcytosine form stable triplexes at neutral pH. *Nucleic Acids Res.* **12**, 6603–6614
12. Povsic, T.J. and Dervan, P.B. (1989) Triple helix formation by oligonucleotides on DNA extended to the physiological pH range. *J. Am. Chem. Soc.* **111**, 3059–3061
13. Xodo, L.E., Manzini, G., Quadrifoglio, F., van der Marel, G.A., and van Boom, J.H. (1991) Effect of 5-methylcytosine on the stability of triple-stranded DNA–a thermodynamic study. *Nucleic Acids Res.* **19**, 5625–5631
14. Ono, A., Tso, P.O.P., and Kan, L.S. (1991) Triplex formation of oligonucleotides containing 2′-*O*-methylpseudoisocytidine in substitution for 2′-deoxycytidine. *J. Am. Chem. Soc.* **113**, 4032–4033
15. Krawczyk, S.H., Milligan, J.F., Wadwani, S., Moulds, C., Froehler, B.C., and Matteucci, M.D. (1992) Oligonucleotide-mediated triple helix formation using an N3-protonated deoxycytidine analog exhibiting pH-independent binding within the physiological range. *Proc. Natl Acad. Sci. USA* **89**, 3761–3764
16. Koh, J.S. and Dervan, P.B. (1992) Design of a nonnatural deoxyribonucleoside for recognition of G:C base pairs by oligonucleotide-directed triple helix formation. *J. Am. Chem. Soc.* **114**, 1470–1478
17. Jetter, M.C. and Hobbs, F.W. (1993) 7,8-Dihydro-8-oxoadenine as a replacement for cytosine in the third strand of triple helices. Triplex formation without hypochromicity. *Biochemistry* **32**, 3249–3254
18. Ueno, Y., Mikawa, M., and Matsuda, A. (1998) Nucleosides and nucleotides. 170. Synthesis and properties of oligodeoxynucleotides containing 5-[N-[2-[N,N-bis(2-aminoethyl)-amino]ethyl] carbamoyl]-2′-deoxyuridine and 5-[N-[3-[N, N-bis(3-aminopropyl)amino]propyl]carbamoyl]-2′-deoxyuridine. *Bioconjug. Chem.* **9**, 33–39
19. Sun, J.S., Giovannangeli, C., Francois, J.C., Kurfurst, R., Montenay-Garestier, T., Asseline, U., Saison-Behmoaras, T., Thuong, N.T., and Helene, C. (1991) Triple-helix formation by alpha oligodeoxynucleotides and alpha oligodeoxynucleotide-intercalator conjugates. *Proc. Natl Acad. Sci. USA* **88**, 6023–6027
20. Mouscadet, J.F., Ketterle, C., Goulaouic, H., Carteau, S., Subra, F., Le Bret, M., and Auclair, C. (1994) Triple helix formation with short oligonucleotide-intercalator conjugates matching the HIV-1 U3 LTR end sequence. *Biochemistry* **33**, 4187–4196
21. Manning, G.S. (1978) The molecular theory of polyelectrolyte solutions with applications to the electrostatic properties of polynucleotides. *Q. Rev. Biophys.* **11**, 179–246
22. Record, M.T. Jr., Anderson, C.F., and Lohman, T.M. (1978) Thermodynamic analysis of ion effects on the binding and conformational equilibria of proteins and nucleic acids: the roles of ion association or release, screening, and ion effects on water activity. *Q. Rev. Biophys.* **11**, 103–178
23. Darnell, J., Lodish, H., and Baltimore, D. (1990) Transport across cell membranes in *Molecular Cell Biology* (Darnell, J., Lodish, H., and Baltimore, D., eds.), pp. 531–578, Scientific American Books, New York
24. Nielsen, P.E., Egholm, M., Berg, R.H., and Buchardt, O. (1991) Sequence-selective recognition of DNA by strand displacement with a thymine-substituted polyamide. *Science* **254**, 1497–1500
25. Nielsen, P.E. (1995) DNA analogues with nonphosphodiester backbones. *Annu. Rev. Biophys. Biomol. Struct.* **24**, 167–183
26. Lacroix, L., Arimondo, P.B., Takasugi, M., Helene, C., and Mergny, J.L. (2000) Pyrimidine morpholino oligonucleotides form a stable triple helix in the absence of magnesium ions. *Biochem. Biophys. Res. Commun.* **270**, 363–369
27. Basye, J., Trent, J.O., Gao, D., and Ebbinghaus, S.W. (2001) Triplex formation by morpholino oligodeoxyribonucleotides in the HER-2/neu promoter requires the pyrimidine motif. *Nucleic Acids Res.* **29**, 4873–4880
28. Stirchak, E.P., Summerton, J.E., and Weller, D.D. (1989) Uncharged stereoregular nucleic acid analogs: 2. Morpholino nucleoside oligomers with carbamate internucleoside linkages. *Nucleic Acids Res.* **17**, 6129–6141
29. Kang, H., Chou, P.J., Johnson, W. C. Jr., Weller, D., Huang, S.B., and Summerton, J.E. (1992) Stacking interactions of ApA analogues with modified backbones. *Biopolymers* **32**, 1351–1363
30. Summerton, J. and Weller, D. (1997) Morpholino antisense oligomers: Design, preparation, and properties. *Antisense Nucleic Acid Drug Dev.* **7**, 187–195
31. Arora, V., Devi, G.R., and Iversen, P.L. (2004) Neutrally charged phosphorodiamidate morpholino antisense oligomers: uptake, efficacy and pharmacokinetics. *Curr. Pharm. Biotechnol.* **5**, 431–439
32. Wickstrom, E., Choob, M., Urtishak, K.A., Tian, X., Sternheim, N., Talbot, S., Archdeacon, J., Efimov, V.A., and Farber, S.A. (2004) Sequence specificity of alternating hydroyprolyl/phosphono peptide nucleic acids against zebrafish embryo mRNAs. *J. Drug Target* **12**, 363–372
33. Amantana, A. and Iversen, P.L. (2005) Pharmacokinetics and biodistribution of phosphorodiamidate morpholino antisense oligomers. *Curr. Opin. Pharmacol.* **5**, 550–555
34. Warfield, K.L., Panchal, R.G., Aman, M.J., and Bavari, S. (2006) Antisense treatments for biothreat agents. *Curr. Opin. Mol. Ther.* **8**, 93–103

35. Karkare, S. and Bhatnagar, D. (2006) Promising nucleic acid analogs and mimics: characteristic features and applications of PNA, LNA, and morpholino. *Appl. Microbiol. Biotechnol.* **71**, 575–586
36. Eisen, J.S. and Smith, J.C. (2008) Controlling morpholino experiments: don't stop making antisense. *Development* **135**, 1735–1743
37. Lyamichev, V.I., Mirkin, S.M., Frank-Kamenetskii, M.D., and Cantor, C.R. (1988) A stable complex between homopyrimidine oligomers and the homologous regions of duplex DNAs. *Nucleic Acids Res.* **16**, 2165–2178
38. Torigoe, H., Ferdous, A., Watanabe, H., Akaike, T., and Maruyama, A. (1999) Poly(L-lysine)-*graft*-dextran copolymer promotes pyrimidine motif triplex DNA formation at physiological pH - thermodynamic and kinetic studies. *J. Biol. Chem.* **274**, 6161–6167
39. Torigoe, H. (2001) Thermodynamic and kinetic effects of N3′→P5′ phosphoramidate modification on pyrimidine motif triplex DNA formation. *Biochemistry* **40**, 1063–1069
40. Torigoe, H. and Maruyama, A. (2005) Synergistic stabilization of nucleic acid assembly by oligo-N3′→P5′ phosphoramidate modification and additions of comb-type cationic copolymers. *J. Am. Chem. Soc.* **127**, 1705–1710
41. Langerman, N. and Biltonen, R.L. (1979) Microcalorimeters for biological chemistry: applications, instrumentation and experimental design. *Methods Enzymol.* **61**, 261–286
42. Biltonen, R.L. and Langerman, N. (1979) Microcalorimetry for biological chemistry: experimental design, data analysis, and interpretation. *Methods Enzymol.* **61**, 287–318
43. Wiseman, T., Williston, S., Brandts, J.F., and Lin, L.N. (1989) Rapid measurement of binding constants and heats of binding using a new titration calorimeter. *Anal. Biochem.* **179**, 131–137
44. Torigoe, H., Shimizume, R., Sarai, A., and Shindo, H. (1999) Triplex formation of chemically modified homopyrimidine oligonucleotides: thermodynamic and kinetic studies. *Biochemistry* **38**, 14653–14659
45. Edwards, P.R., Gill, A., Pollard-Knight, D.V., Hoare, M., Buckle, P.E., Lowe, P.A., and Leatherbarrow, R.J. (1995) Kinetics of protein-protein interactions at the surface of an optical biosensor. *Anal. Biochem.* **231**, 210–217
46. Bates, P.J., Dosanjh, H.S., Kumar, S., Jenkins, T.C., Laughton, C.A., and Neidle, S. (1995) Detection and kinetic studies of triplex formation by oligodeoxynucleotides using real-time biomolecular interaction analysis (BIA). *Nucleic Acids Res.* **23**, 3627–3632
47. Manzini, G., Xodo, L.E., Gasparotto, D., Quadrifoglio, F., van der Marel, G.A., and van Boom, J.H. (1990) Triple helix formation by oligopurine-oligopyrimidine DNA fragments. Electrophoretic and thermodynamic behavior. *J. Mol. Biol.* **213**, 833–843
48. Edelhoch, H. and Osborne, J.C. Jr. (1976) The thermodynamic basis of the stability of proteins, nucleic acids, and membranes. *Adv. Protein Chem.* **30**, 183–250
49. Cheng, Y.K. and Pettitt, B.M. (1992) Stabilities of double- and triple-strand helical nucleic acids. *Prog. Biophys. Mol. Biol.* **58**, 225–257
50. Kamiya, M., Torigoe, H., Shindo, H., and Sarai, A. (1996) Temperature dependence and sequence specificity of DNA triplex formation: An analysis using isothermal titration calorimetry. *J. Am. Chem. Soc.* **118**, 4532–4538
51. Shafer, R.H. (1998) Stability and structure of model DNA triplexes and quadruplexes and their interactions with small ligands. *Prog. Nucleic Acid Res. Mol. Biol.* **59**, 55–94
52. Rougee, M., Faucon, B., Mergny, J.L., Barcelo, F., Giovannangeli, C., Garestier, T., and Helene, C. (1992) Kinetics and thermodynamics of triple-helix formation: effects of ionic strength and mismatches. *Biochemistry* **31**, 9269–9278